

Vehicle Networks for Gradient Descent in a Sampled Environment

Ralf Bachmayer and Naomi Ehrich Leonard¹
Department of Mechanical and Aerospace Engineering
Princeton University
Princeton, NJ 08544 USA
ralf@princeton.edu, naomi@princeton.edu

Abstract

Fish in a school efficiently find the densest source of food by individually responding not only to local environmental stimuli but also to the behavior of nearest neighbors. It is of great interest to enable a network of autonomous vehicles to function similarly as an intelligent sensor array capable of climbing or descending gradients of some spatially distributed signal. We formulate and study a coordinated control strategy for a group of autonomous vehicles to descend or climb an environmental gradient using measurements of the environment together with relative position measurements of nearest neighbors. Each vehicle is driven by an estimate of the local environmental gradient together with control forces, derived from artificial potentials, that maintain uniformity in group geometry.

1 Introduction

We propose a coordinated control strategy for multi-vehicle gradient descent (ascent) in a sampled environment. Vehicle networks that can efficiently climb gradients are of great interest in missions such as search and map where a spatially distributed environmental signal is to be mapped or its source is to be found. Applications exist from deep space to the deep sea. For instance, vehicles that can climb mineral plumes and/or temperature gradients would improve the success of searches for hydrothermal vents deep in the sea.

In this context, a vehicle network has a number of important advantages over a single large vehicle. The large vehicle could be outfitted with distributed sensors so that local gradients could be computed. However, the sensor array would then be rigid and therefore there would be little ability to adapt the array configuration to the environment. Further, failure of the vehicle would mean failure of the entire mission.

A coordinated network of smaller and simpler individual vehicles, on the other hand, could provide an adaptive and reconfigurable distributed sensor array. Further, robustness to a single vehicle failure would be improved; in our approach we avoid assigning any ordering to the vehicles so the vehicles are interchangeable and the importance of any single vehicle is minimized.

Our goal is to design a coordinating control strategy that achieves efficient and adaptive group capabilities from simple rules at the individual vehicle level, much like emergent intelligence in schools of fish. Schools of fish and other animal aggregations forage and evade predators with great skill [9, 10]. A key ingredient to the success of these group behaviors is that each individual responds to the behavior of its nearest neighbors.

Gradient following by autonomous vehicle systems inspired by bacterial chemotaxis has been explored in [2, 5]. In [4], an approach similar to ours is taken in which individuals balance their own gradient descent with inter-vehicle attraction and repulsion forces. The approach in [4] differs from ours; for example, the authors in [4] restrict to each vehicle knowing the full gradient at its location and knowing the relative position of each of the other vehicles. In [8] a virtual leader approach to gradient climbing is taken and a rule is proposed for adapting the desired inter-vehicle distance as a function of the measured gradient field and a bound on measurement error.

In [1] we first outlined our gradient climbing approach which uses control forces that sum approximations of the local gradient with inter-vehicle control forces derived from artificial potentials. The approximation of the local gradient is based on a single sensor per vehicle; each vehicle is assumed to be able to measure the gradient only in the direction of motion. In general, a vehicle that descends a gradient using only this projected gradient information will not find the global minimum of the gradient field but instead the minimum along the line defined by the vehicle's initial velocity. However, the inter-vehicle forces that we introduce provide the necessary implicit communication to drive the group as a whole to the global minimum (or maximum) of the sampled environmental gradient field.

¹Research partially supported by the Office of Naval Research under grants N00014-98-1-0649 and N00014-01-1-0526, by the National Science Foundation under grant CCR-9980058 and by the Air Force Office of Scientific Research under grant F49620-01-1-0382.

In [1] we also described our 3D, multi-vehicle testbed.

In §2 we describe our vehicle model and the approach to coordination of vehicles using artificial potentials. In §3 we present our coordinated strategy for gradient descent (ascent) in the case that each individual vehicle can measure the gradient at its current position. In §4 we describe our approach for the more compelling and more challenging problem of a vehicle group in which each individual vehicle has only a single sensor. We demonstrate our approach with simulations.

2 Coordinating Control with Interaction Potentials

Each vehicle in the network is modelled as a point mass with fully actuated dynamics. Extension to underactuated systems is possible. For example, in [6], the authors consider the dynamics of an off-axis point on a nonholonomic robot and use feedback linearization to transform the resulting system dynamics into fully actuated double integrator equations of motion.

For our presentation of gradient descent we specialize to planar motions, and let the position of the i th vehicle in a group of N vehicles be given by a vector $\mathbf{x}_i \in \mathbb{R}^2$, $i = 1, \dots, N$. The control force on the i th vehicle is given by $\mathbf{u}_i \in \mathbb{R}^2$. Since we assume full actuation, the dynamics can be written for $i = 1, \dots, N$

$$\ddot{\mathbf{x}}_i = \mathbf{u}_i.$$

To coordinate the motion of the vehicles we introduce inter-vehicle artificial potentials. This follows the general framework for using artificial potentials for coordinated control described in [7]. For each pair of vehicles i and j , we define a potential $V_I(\mathbf{x}_{ij})$ where

$$\mathbf{x}_{ij} = \mathbf{x}_i - \mathbf{x}_j.$$

The corresponding interaction force is derived from the gradient of the artificial potential V_I . The force applied to the i th vehicle is

$$-\mathbf{F}_I(\mathbf{x}_{ij}) = -\nabla V_I(\mathbf{x}_{ij})$$

where the gradient is taken with respect to \mathbf{x}_i . Accordingly, the forces on the vehicles, i and j , generated from this potential are equal and opposite,

$$\mathbf{F}_I(\mathbf{x}_{ij}) = -\mathbf{F}_I(\mathbf{x}_{ji}). \quad (2.1)$$

The shape of the potential can be designed to reflect the behavior widely observed in animal groups: individuals are attracted to each other if they are far apart and repelled if they are very close. The simplest model for this kind of behavior is a linear spring force derived from a quadratic potential, with a relaxation distance $d_0 > 0$ and spring constant $k_s > 0$:

$$V_I(\mathbf{x}_{ij}) = \frac{1}{2}k_s(\|\mathbf{x}_{ij}\| - d_0)^2. \quad (2.2)$$

One major shortcoming of the spring force is the increasing magnitude of the force of attraction with increasing distance between vehicles. This is inconsistent with observations of animal groups which suggest each individual is only influenced by a set of nearest neighbors. A second shortcoming of the linear spring interaction model is a finite repulsive force when two vehicles come arbitrarily close to each other. To avoid collisions it is desirable instead to let the repelling force get arbitrarily large.

The nonlinear spring potential used in [7] (and ones like it) does not have these two shortcomings:

$$V_I(\mathbf{x}_{ij}) = k_s \left(\ln \|\mathbf{x}_{ij}\| + \frac{d_0}{\|\mathbf{x}_{ij}\|^2} \right). \quad (2.3)$$

The force of attraction goes to zero with increasing distance between vehicles and the force of repulsion goes to infinity as this distance approaches zero. Further, as presented in [7], this potential can be (smoothly or non-smoothly) made constant above some prescribed inter-vehicle distance d_1 so that the interaction force is zero for $\|\mathbf{x}_{ij}\| > d_1$.

In this paper we will prove a number of results for a general choice of potential, but for simplicity reasons, we will draw some specific conclusions in the case of inter-vehicle linear spring potentials.

We apply the identical control law to each vehicle which yields a system of N identical vehicles with the following dynamics for each vehicle i :

$$\ddot{\mathbf{x}}_i = - \sum_{j=1, j \neq i}^N \mathbf{F}_I(\mathbf{x}_{ij}) - k_d \dot{\mathbf{x}}_i. \quad (2.4)$$

Note that we have included a damping term dependent only on absolute velocity with scalar coefficient $k_d > 0$. One could also introduce a term that depends on relative velocity between pairs of vehicles.

Let the Lyapunov function be the sum of the kinetic and potential energies of the system:

$$V = \frac{1}{2} \sum_{i=1}^N \dot{\mathbf{x}}_i \cdot \dot{\mathbf{x}}_i + \sum_{i=1}^{N-1} \sum_{j=i+1}^N V_I(\mathbf{x}_{ij}).$$

The time derivative of V is

$$\dot{V} = \sum_{i=1}^N \dot{\mathbf{x}}_i \cdot \ddot{\mathbf{x}}_i + \sum_{i=1}^{N-1} \sum_{j=i+1}^N \mathbf{F}_I(\mathbf{x}_{ij}) \cdot \dot{\mathbf{x}}_{ij}. \quad (2.5)$$

If we substitute (2.4) for $\ddot{\mathbf{x}}_i$ into (2.5), we get

$$\dot{V} = -k_d \sum_{i=1}^N \|\dot{\mathbf{x}}_i\|^2. \quad (2.6)$$

This result guarantees stability of the group of N -vehicles in the absence of additional external forces. The equilibria of the group have to satisfy

$$\sum_{j=1, j \neq i}^N \mathbf{F}_I(\mathbf{x}_{ij}) = \mathbf{0}$$

for $i = 1, \dots, N$. For a further discussion of stability of formation equilibria the reader is referred to [7].

3 Gradient Descent with Local Gradient Information

In this section we describe vehicle network gradient descent (ascent) in an environmental field in the case each vehicle has enough sensors to measure the gradient of the field at its current position. The gradient descent control term is complemented with the inter-vehicle forces described above to enforce coordinated gradient descent.

For the single vehicle case, with $\ddot{\mathbf{x}} = \mathbf{u}$, we define the control law to be

$$\mathbf{u} = -k_d \dot{\mathbf{x}} - \kappa \nabla T(\mathbf{x}), \quad (3.1)$$

where $T : \mathbb{R}^2 \rightarrow \mathbb{R}$ is the gradient field and $k_d > 0$ and κ are constant control parameters. In the case of a gradient field $T(\mathbf{x})$ with a strict minimum at the origin, asymptotic stability of the origin is easily proved using the Lyapunov function

$$V(\mathbf{x}, \dot{\mathbf{x}}) = \frac{1}{2} \dot{\mathbf{x}} \cdot \dot{\mathbf{x}} + \kappa T(\mathbf{x})$$

with $\kappa > 0$. If the origin is a unique, global minimum, then global asymptotic stability results are possible. Analogous results hold for gradient climbing in the case that T has a strict maximum at the origin if one takes $\kappa < 0$.

If we use the same control law for each vehicle plus the interaction forces $\mathbf{F}_I(\mathbf{x}_{ij})$ on a group of N vehicles we obtain the following system of equations:

$$\ddot{\mathbf{x}}_i = -\kappa \nabla T(\mathbf{x}_i) - k_d \dot{\mathbf{x}}_i - \sum_{j=1, j \neq i}^N \mathbf{F}_I(\mathbf{x}_{ij}). \quad (3.2)$$

As in the case of the N -vehicle system without external forcing, we let the Lyapunov function be the sum of the kinetic and potential energies of the system. Here, however, we include the field T in the potential energy:

$$V = \frac{1}{2} \sum_{i=1}^N (\dot{\mathbf{x}}_i \cdot \dot{\mathbf{x}}_i + \kappa T(\mathbf{x}_i)) + \sum_{i=1}^{N-1} \sum_{j=i+1}^N V_I(\mathbf{x}_{ij}). \quad (3.3)$$

The time derivative of V is

$$\begin{aligned} \dot{V} = & \sum_{i=1}^N \dot{\mathbf{x}}_i \cdot \ddot{\mathbf{x}}_i + \kappa \sum_{i=1}^N \nabla T(\mathbf{x}_i) \cdot \dot{\mathbf{x}}_i \\ & + \sum_{i=1}^{N-1} \sum_{j=i+1}^N \mathbf{F}_I(\mathbf{x}_{ij}) \cdot \dot{\mathbf{x}}_{ij}. \end{aligned} \quad (3.4)$$

If we substitute (3.2) for $\ddot{\mathbf{x}}_i$ into (3.4), we get

$$\dot{V} = -k_d \sum_{i=1}^N \|\dot{\mathbf{x}}_i\|^2. \quad (3.5)$$

Proposition 3.1 *Let T be a gradient field and consider a group of N vehicles with the control law specified in (3.2). Then, an equilibrium corresponding to a located formation that is a strict minimizer of $\kappa \sum_{i=1}^N T(\mathbf{x}_i) + \sum_{i=1}^{N-1} \sum_{j=i+1}^N V_I(\mathbf{x}_{ij})$ will be a stable equilibrium for the coupled dynamics.*

Depending upon the extent of the symmetry in the controlled dynamics, application of LaSalle's Invariance principle may show convergence to a set of non-isolated equilibria. In this case asymptotic stability results will typically be proved modulo the symmetry directions. We illustrate this with an example below (see also [7]).

The minimum of the sum of all inter-vehicle potentials and the environmental potential can be found by solving for the equilibria of (3.2). This gives

$$\mathbf{0} = -\kappa \nabla T(\mathbf{x}_i) - \sum_{j=1, j \neq i}^N \mathbf{F}_I(\mathbf{x}_{ij}), \quad i = 1, \dots, N. \quad (3.6)$$

Since $\mathbf{F}_I(\mathbf{x}_{ij}) = -\mathbf{F}_I(\mathbf{x}_{ji})$ we obtain the following condition for the equilibria by summing (3.6) over i :

$$\sum_{i=1}^N \nabla T(\mathbf{x}_i) = \mathbf{0}. \quad (3.7)$$

Proposition 3.2 *Suppose that T is a radially symmetric gradient field $T = T(\|\mathbf{x}\|)$ with strict global minimum at $\mathbf{x} = \mathbf{0}$. Suppose further that $T(\|\mathbf{x}\|)$ is strictly increasing, i.e., $\partial T(\|\mathbf{x}\|)/\partial \|\mathbf{x}\| > 0$ for all $\|\mathbf{x}\| > 0$. Then, the convex hull of any equilibrium formation of the controlled dynamics (3.2) for N vehicles contains the minimum of the field $\mathbf{x} = \mathbf{0}$.*

Proof. For the given field T , the equilibrium condition (3.7) implies

$$\sum_{i=1}^N a_i(\|\mathbf{x}_i\|) \mathbf{x}_i = \mathbf{0}$$

where $a_i > 0$ for $\|\mathbf{x}_i\| > 0$. If $\mathbf{x}_i = \mathbf{0}$ for some i then $\mathbf{x} = \mathbf{0}$ is trivially in the convex hull of the vehicle positions. So, consider the case in which $\mathbf{x}_i \neq \mathbf{0} \forall i$. Let $a = a_1 + \dots + a_n > 0$ and $b_i = a_i/a$. Then, $b_1 + \dots + b_n = 1$ and so

$$\sum_{i=1}^N b_i(\|\mathbf{x}_i\|) \mathbf{x}_i = \mathbf{0}$$

which by definition implies that $\mathbf{0}$ is in the convex hull of the equilibrium. \square

We note that this result and similar results that follow can be stated and proved analogously for the gradient climbing problem, i.e., where $T(\mathbf{x})$ has a maximum at $\mathbf{x} = \mathbf{0}$. Some useful results are now proved in the case of a quadratic gradient field. We note that a more complicated gradient field can be approximated near a minimum by such a quadratic field.

Corollary 3.3 Consider the assumptions of Proposition 3.2 and suppose that $T(\|\mathbf{x}\|) = \frac{1}{2}\mathbf{x} \cdot P\mathbf{x}$, $P > 0$ and symmetric. Then, $\mathbf{x} = \mathbf{0}$ is the center of mass of any equilibrium formation.

Proof. The equilibrium condition (3.7) implies

$$P \sum_{i=1}^N \mathbf{x}_i = \mathbf{0},$$

i.e., the origin is the center of mass of N vehicles of identical mass. \square

In this case, the dynamics of the center of mass are decoupled from the rest of the dynamics. To see this define a change of coordinates

$$(\mathbf{x}_1, \mathbf{x}_2, \dots, \mathbf{x}_N) \mapsto (\mathbf{x}_c, \mathbf{x}_{12}, \mathbf{x}_{23}, \dots, \mathbf{x}_{(N-1)N}),$$

where

$$\mathbf{x}_c = \frac{1}{N} \sum_{i=1}^N \mathbf{x}_i.$$

Then, using (3.2) we get

$$\ddot{\mathbf{x}}_c = \frac{1}{N} \sum_{i=1}^N \ddot{\mathbf{x}}_i = -\kappa P \mathbf{x}_c - k_d \dot{\mathbf{x}}_c \quad (3.8)$$

Proposition 3.4 Let $T(\|\mathbf{x}\|) = \frac{1}{2}\mathbf{x} \cdot P\mathbf{x}$, $P > 0$, and consider the controlled group dynamics given by (3.2). Then, for any initial condition, the center of mass of the group converges exponentially to the origin.

Proof. The dynamics of the center of mass of the vehicle group are given by (3.8) and $\mathbf{x}_c = \mathbf{0}$ is a globally exponentially stable equilibrium for these dynamics. \square

In this case, the system's center of mass behaves like the single vehicle case independent of the relative motion of the individual vehicles. It is of interest to investigate the dynamics of the center of mass and the relative motion of vehicles for more general gradient fields. This is the subject of continuing work.

Next, we examine two special cases for illustration. In both of these cases we take $T(\|\mathbf{x}\|) = \frac{1}{2}\|\mathbf{x}\|^2$ and we take the inter-vehicle potential to be the linear spring potential (2.2). We look at the multi-vehicle cases $N = 2$ and $N = 3$.

Proposition 3.5 Let $N = 2$, $T(\|\mathbf{x}\|) = \frac{1}{2}\|\mathbf{x}\|^2$ and V_I be given by (2.2). The controlled dynamics (3.2) globally asymptotically converge to an equilibrium in the set that consists of the two vehicles at rest on antipodal points of a circle centered at the origin with radius

$$r = \frac{k_s d_0}{\kappa + 2k_s}.$$

Proof. The equilibria for the closed-loop dynamics satisfy

$$\begin{aligned} \mathbf{0} &= -\kappa \mathbf{x}_1 - k_s \mathbf{x}_{12} \left(1 - \frac{d_0}{\|\mathbf{x}_{12}\|}\right) \\ \mathbf{0} &= -\kappa \mathbf{x}_2 - k_s \mathbf{x}_{21} \left(1 - \frac{d_0}{\|\mathbf{x}_{21}\|}\right). \end{aligned} \quad (3.9)$$

Summing these two equations gives $\mathbf{x}_1 = -\mathbf{x}_2$. Without loss of generality let $\mathbf{x}_1 = (r, 0)$ and $\mathbf{x}_2 = (-r, 0)$. Then, plugging this into either of the equations (3.9) gives

$$2k_s r - k_s d_0 + \kappa r = 0$$

which can be solved for r as in the proposition. Any equilibrium in this set minimizes the total potential and therefore this is a set of stable equilibria following Proposition 3.1. Note that this set constitutes the only equilibria for this system. Since $\dot{\mathbf{x}}_i = \mathbf{0}$ for all i when $\dot{V} = 0$ from (3.5), application of the LaSalle's Invariance principle guarantees convergence to one of the equilibria from this set. \square

The case of $N = 3$ is similar to the $N = 2$ case. However, in this case there is a family of unstable equilibria in addition to a family of stable equilibria.

Proposition 3.6 Let $N = 3$, $T(\|\mathbf{x}\|) = \frac{1}{2}\|\mathbf{x}\|^2$ and V_I be given by (2.2). For every initial condition except for a set of measure zero, the controlled dynamics (3.2) asymptotically converge to an equilibrium in the set that consists of the three vehicles at rest in an equilateral triangle centered at the origin. Each vehicle is a distance r from the origin where

$$r = \frac{\sqrt{3}k_s d_0}{\kappa + 3k_s}.$$

Proof. The proof begins similarly to the proof of Proposition 3.5. Equilibria must satisfy the equations

$$\begin{aligned} \frac{\kappa}{k_s} \nabla T(\mathbf{x}_1) &= -\mathbf{x}_{12} \left(1 - \frac{d_0}{\|\mathbf{x}_{12}\|}\right) - \mathbf{x}_{13} \left(1 - \frac{d_0}{\|\mathbf{x}_{13}\|}\right) \\ \frac{\kappa}{k_s} \nabla T(\mathbf{x}_2) &= -\mathbf{x}_{21} \left(1 - \frac{d_0}{\|\mathbf{x}_{21}\|}\right) - \mathbf{x}_{23} \left(1 - \frac{d_0}{\|\mathbf{x}_{23}\|}\right) \\ \frac{\kappa}{k_s} \nabla T(\mathbf{x}_3) &= -\mathbf{x}_{31} \left(1 - \frac{d_0}{\|\mathbf{x}_{31}\|}\right) - \mathbf{x}_{32} \left(1 - \frac{d_0}{\|\mathbf{x}_{32}\|}\right). \end{aligned}$$

These equations can be solved to find two families of equilibria. One family of equilibria is the solution consisting of each vehicle at a vertex of an equilateral triangle inscribing a circle of radius

$$\rho_A = \frac{\sqrt{3}k_s d_0}{\kappa + 3k_s} \quad (3.10)$$

centered at the origin. This type of equilibrium is shown on the right side of Figure 3.1.

A second set of equilibria takes the form

$$\|\mathbf{x}_i\| = \rho_B = \frac{2k_s d_0}{\kappa + 3k_s}, \quad \mathbf{x}_j = -\mathbf{x}_i, \quad \mathbf{x}_k = \mathbf{0} \quad (3.11)$$

as illustrated on the left of Figure 3.1.

Linearizing the controlled dynamics (3.2) at the equilibrium points reveals that the equilateral triangle configuration is stable while the collinear solution

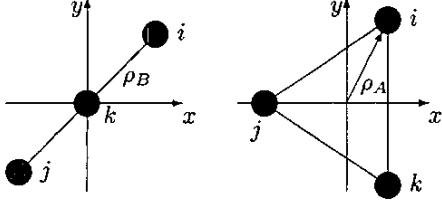


Figure 3.1: Fixed point solutions for the 3 vehicle problem. Left the (unstable) collinear solution and right the stable equilateral triangle solution.

is unstable with the following eigenvalues:

$$\lambda = -\frac{1}{2} \begin{bmatrix} k_d \pm \sqrt{k_d^2 - 12k_s - 4\kappa} \\ k_d \pm \sqrt{k_d^2 - 30k_s - 10\kappa} \\ 0 \\ k_d \pm \sqrt{k_d^2 - 4\kappa} \\ 2k_d \\ k_d \pm \sqrt{k_d^2 + 6k_s + 2\kappa} \\ k_d \pm \sqrt{k_d^2 - 24k_s - 8\kappa} \end{bmatrix}. \quad (3.12)$$

For $k_s \kappa \neq 0$, the eigenvalue $\lambda = -1/2(k_d - \sqrt{k_d^2 + 6k_s + 2\kappa})$ has positive real part. The single zero eigenvalue corresponds to the S^1 symmetry in the system dynamics; both the triangle equilibrium and the collinear equilibrium are hyperbolic for the reduced (eleven) dynamical equations. Thus, for the reduced equations the triangle equilibrium is almost globally asymptotically stable. In the unreduced setting, all trajectories, except for the family of collinear solutions, converge to a triangle solution. \square

4 Gradient Descent with Projected Gradient Information

In §3 we assumed each vehicle could measure the local gradient of T . In the remainder of this paper we constrain the system to a single sensor per vehicle and assume we can make use of the time history of the measurement on each vehicle. The single point sensor measurements do not allow for a full (2D) spatial gradient measurement for a given vehicle. Instead, the measurements provide information about the gradient along the vehicle's path. We assume we can use the successive measurements taken along a vehicle's path to compute the projection of the spatial gradient onto the normalized vehicle velocity vector, $e_{\dot{x}} = \frac{\dot{x}}{\|\dot{x}\|}$, i.e.,

$$\nabla T_P(x, \dot{x}) := \left(\nabla T(x) \cdot \frac{\dot{x}}{\|\dot{x}\|} \right) \frac{\dot{x}}{\|\dot{x}\|} = (\nabla T(x) \cdot e_{\dot{x}}) e_{\dot{x}}. \quad (4.1)$$

Here, we investigate the same control law as described in §3 except we replace the local gradient measurement by the projected gradient. The dynamics of

vehicle i are given by

$$\ddot{x}_i = -\kappa \nabla T_P(x_i, \dot{x}_i) - k_d \dot{x}_i - \sum_{j=1, j \neq i}^N F_I(x_{ij}). \quad (4.2)$$

Consider first the case of a single vehicle with position vector x . Note that for $\dot{x} = 0$ the control law is not defined because the projected gradient is not defined. However, in the single vehicle case, the control law (defined for $\dot{x} \neq 0$) restricts the vehicle to 1D motion since every force term is parallel to the initial velocity. Assuming no perturbations transverse to this direction and a nontrivial initial condition, the limit

$$\lim_{\dot{x} \rightarrow 0} \nabla T_P(x, \dot{x}) \quad (4.3)$$

exists. In particular, the limit of the projected gradient will be in the direction parallel to the initial velocity.

In order to accommodate the discontinuous right hand side of (4.2) for more general analysis, we replace the dynamical system (4.2) with the following differential inclusion:

$$\ddot{x} \in F(x, \dot{x}) \quad (4.4)$$

$$F(x, \dot{x}) = \begin{cases} -\kappa \nabla T_P(x, \dot{x}) - k_d \dot{x} & \forall \dot{x} \neq 0 \\ -\kappa (\nabla T(x) \cdot e_{\dot{x}}^*) e_{\dot{x}}^* & \dot{x} = 0 \end{cases} \quad (4.5)$$

with

$$e_{\dot{x}}^* \in E = \{e_{\dot{x}} \in \mathbb{R}^2 \mid \|e_{\dot{x}}\| = 1\}.$$

A differential inclusion constructed in this way allows us to determine the stability properties of the system by examining the stability properties in the continuous domain (see Filippov [3]).

For example, for the single vehicle case we construct a Lyapunov function

$$V = \frac{1}{2} \dot{x} \cdot \dot{x} + \kappa T(x)$$

Then,

$$\dot{V} = \dot{x} \cdot \ddot{x} + \kappa \nabla T(x) \cdot \dot{x} = -k_d \|\dot{x}\|^2 \quad (4.6)$$

since

$$\dot{x} \cdot \nabla T_P(x, \dot{x}) = \nabla T(x) \cdot \dot{x}.$$

This implies the velocity of the vehicle goes asymptotically to zero.

The fixed points of the system have to satisfy

$$-\kappa (\nabla T(x) \cdot e_{\dot{x}}^*) e_{\dot{x}}^* = 0. \quad (4.7)$$

In general there are many equilibria since $e_{\dot{x}}^*$ could be any unit vector. However, if we choose $e_{\dot{x}}^*$ to be the limit of $e_{\dot{x}}$ (in the case of no transverse perturbations and nontrivial initial condition), then the dynamics of the single vehicle are restricted to a line. In this case, x will converge to the (local) minimum of the gradient field *projected in the direction of initial velocity* since

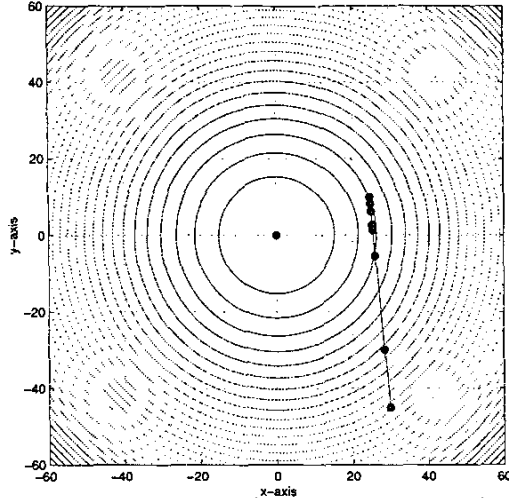


Figure 4.1: Simulation of single vehicle with single sensor.

$\nabla T(x) \cdot e_x^* = 0$ at the minimum of the gradient field projected along this line. Simulations support these conclusions as shown in Figure 4.1. The figure shows the vehicle converging to $\nabla T_P(x) = 0$ along its initial path. The gradient field is $\frac{1}{2}\|x\|^2$.

In the case of $N > 1$ vehicles, the differential inclusion can be constructed as

$$\ddot{x}_i \in F(x_i, \dot{x}_i)$$

where

$$F(x_i, \dot{x}_i) = \begin{cases} \text{rhs of (4.2)} & \forall \dot{x}_i \neq 0 \\ -\kappa(\nabla T(x_i) \cdot e_{\dot{x}_i}^*)e_{\dot{x}_i}^* & \dot{x}_i = 0. \\ -\sum_{j=1, j \neq i}^n F_I(x_{ij}) & \end{cases}$$

Further, using the Lyapunov function defined by (3.3), the derivative of V is given by (3.4). Substituting for \ddot{x}_i as given by (4.2) still gives the result (3.5), and we can conclude that the velocity of each vehicle goes to zero asymptotically. In a future work we will present the stable equilibrium solutions in the multi-vehicle case and the details of the stability proof. It may not necessarily be the case that for each vehicle in the multi-vehicle case that the limit (4.3) exists. The plot of Figure 4.2 illustrates the convergence of a group of three vehicles in a gradient field $T(x) = 1/2\|x\|^2$ with linear spring force between each pair of vehicles. The plot shows the vehicles converging to the global minimum $x = 0$.

This and other simulations that we have run are very encouraging. They suggest the power of the vehicle network over the uncoordinated collection of individual vehicles. With limited sensing the individual vehicles won't in general find the minimum of the field. On the other hand, for the examples we have simulated, the multi-vehicle system (with single sensors) can find the global minimum.

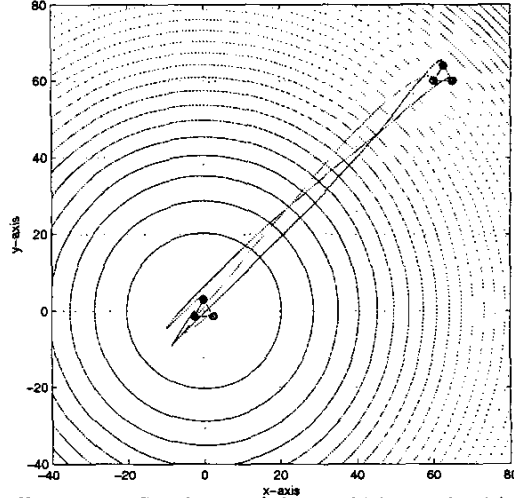


Figure 4.2: Simulation of three vehicles, each with single sensor.

5 Acknowledgements

The authors would like to thank Eduardo Sontag and Luc Moreau for stimulating and insightful discussions on this subject.

References

- [1] R. Bachmayer and N.E. Leonard. Experimental test-bed for multi-vehicle control, navigation and communication. In *Proc. 12th Int. Symp. Unmanned Untethered Submersible Tech.*, 2001.
- [2] E. Burian, D. Yoerger, A. Bradley, and H. Singh. Gradient search with autonomous underwater vehicle using scalar measurements. *Proc. IEEE OES AUV Conf.*, 1996.
- [3] A. F. Filippov. *Differential Equations with Discontinuous Righthand Sides*. Kluwer Academic Press, Dordrecht, The Netherlands, 1988.
- [4] V. Gazi and K. Passino. Stability analysis of social foraging swarms. Preprint, February 2002.
- [5] D. A. Hoskins. A least action approach to collective behavior. *Microrobotics and Micromechanical Systems*, Proc. SPIE 2593:108–120, 1995. L. E. Parker, Editor.
- [6] J. Lawton, B. Young, and R. Beard. A decentralized approach to elementary formation maneuvers. *IEEE Trans. Robotics and Automation*, 2002. To appear.
- [7] N.E. Leonard and E. Fiorelli. Virtual leaders, artificial potentials and coordinated control of groups. In *Proc. 40th IEEE CDC*, pages 2968–2973, 2001.
- [8] P. Ögren, E. Fiorelli, and N.E. Leonard. Formations with a mission: Stable coordination of vehicle group maneuvers. In *Proc. 15th MTNS*, 2002.
- [9] A. Okubo. Dynamical aspects of animal grouping: Swarms, schools, flocks and herds. *Advances in Biophysics*, pages 1–94, 1985.
- [10] J. K. Parrish and W. H. Hammer, editors. *Animal Groups in Three Dimensions*, page 378. Cambridge University Press, 1997.